Enhancing the capacity of supercapacitive swing adsorption CO_2 capture by tuning charging protocols and pH

Trevor B. Binford, Grace Mapstone, Israel Temprano, Alexander C. Forse*

Department of Chemistry, University of Cambridge, Lensfield Road, CB2 1EW, UK

*corresponding author, E-mail: acf50@cam.ac.uk

ABSTRACT: Supercapacitive swing adsorption (SSA) is a recently discovered electrochemically driven CO_2 capture technology that promises significant efficiency improvements over traditional methods. A limitation of this approach is the relatively low CO_2 adsorption capacity, and the underlying molecular mechanisms of SSA remain poorly understood, hindering optimization. Here we present a new device architecture for simultaneous electrochemical and gas-adsorption measurements, and use it to investigate the effects of charging protocols and electrolyte pH on SSA performance. We show that although pH 7 is already near optimal, altering the voltage applied to charge the SSA device can significantly improve performance. Charging the gas-exposed electrode positively rather than negatively increases CO_2 adsorption capacity and causes CO_2 desorption rather than adsorption with charging. We also show that switching the voltage between positive and negative values further increases CO_2 capacity. Previously proposed mechanisms of the SSA effect fail to explain these phenomena, so we present a new mechanism based on movement of CO_2-derived species into and out of electrode micropores. Overall, this work advances our knowledge of electrochemical CO_2 adsorption by supercapacitors, potentially leading to devices with increased uptake capacity and efficiency.

Climate change is one of the greatest challenges the world faces in the 21st century. The Intergovernmental Panel on Climate Change (IPCC) estimates that to limit global temperature increase to 1.5 °C above pre-industrial levels, the world needs to achieve net carbon neutrality by 2050.[1] Although expanding renewable energy will be vital to reach this goal,[2] certain industries such as cement manufacturing are intrinsically linked to CO_2 emissions, while in the short term, fossil fuels will continue to be vital to the world economy. Carbon dioxide capture at point sources is currently one of the cheapest ways to reduce industrial greenhouse gas emissions,[3] and can help to close this gap. The IPCC asserts that all pathways to limit global warming to 1.5 °C will require "carbon dioxide removal (CDR) on the order of 100-1000 $GtCO_2$ over the 21st century",[1] where CDR refers to removal of carbon dioxide from the atmosphere rather than point emissions. Other estimates require annual CO_2 capture of 75-175 $MtCO_2$ in the UK alone to meet net-zero targets.[4]

The best-developed carbon capture technique is solvent scrubbing, where aqueous amine solvents are used to selectively absorb CO_2. Heating the solvent, known as a temperature swing, drives CO_2 out for storage and returns the system to its original state.[5] However, raising the temperature of a large volume of solvent requires substantial energy input, limiting efficiency. Amine solvents can also corrode equipment, be poisoned by impurities in the flue gas, or escape as vapor to cause environmental damage.[6] These issues mean that electrochemical swing adsorption, an emerging CO_2 capture technology driven by electrochemistry, may have potential advantages.[7–12]

Supercapacitive swing adsorption (SSA) is a form of electrochemical swing CO_2 capture based on charging supercapacitors.[13] One electrode of the supercapacitor is exposed to a CO_2-containing gas and the other is completely soaked in electrolyte. When the supercapacitor is charged, CO_2 is selectively adsorbed from the gas (and released with discharging). The effect has primarily been studied with activated carbon electrodes and aqueous sodium chloride electrolyte,[14–16] an affordable and environmentally-friendly model system.

This system, however, has a limited CO_2 capacity compared to amine scrubbing, typically ~60 mmol of CO_2 per kg of adsorbent,[14] while amine scrubbing can reach ~800 mmol of CO_2 per kg of solvent.[17] Performance has been improved by adding ion exchange membranes above the electrodes to increase the selectivity for the CO_2-derived ions H^+, HCO_3^- in the electric double layer.[11,18] Little energy is wasted adsorbing electrolyte ions, so the membrane capacitive deionization approach is significantly more energy efficient. However, the added cost and complexity from the ion-exchange membranes is a drawback compared to the simple SSA approach. Besides low capacities, an additional challenge is the

lack of fundamental understanding of electrochemical CO_2 capture by supercapacitors. To address these challenges, here we explore new charging protocols and experimental set-ups to obtain new insights into the mechanisms of supercapacitive swing adsorption.

To monitor the electrochemical adsorption of CO_2 by supercapacitors we adopted an electrochemical cell equipped with a gas pressure sensor for monitoring gas uptake and release[19] (Figure 1, also see Supplementary Information). Briefly, symmetric activated carbon-based supercapacitors (YP50-F carbon, Kuraray) with 1 M NaCl (aq.) electrolyte are housed in a gas-tight Swagelok cell assembly. The top electrode is directly in contact with a gas reservoir filled with pure CO_2.

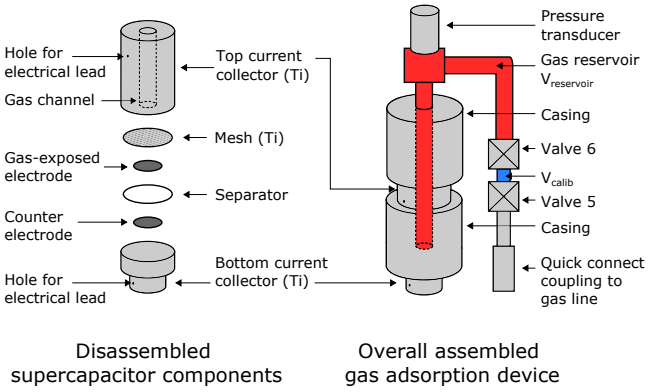

Figure 1. Schematic diagram of the supercapacitive swing adsorption device used to monitor gas pressure during electrochemical measurements.

To date, the bulk of the SSA literature has focused on charging the supercapacitor with the negative electrode exposed to the gas, which we will term negative charging. We are only aware of one published experiment in which the positive electrode is exposed to the gas (positive charging).[13] Therefore, we examined the effect of both negative and positive charging (representative data shown in Figure 2 and the overall experiment in Figure S1).

Initial experiments with negative charging revealed reversible electrochemical adsorption (Figure 2a). As in the literature,[13] we observed CO_2 adsorption when carrying out negative charging *i.e.* when the cell voltage is varied between 0 and –1 V, CO_2 is adsorbed by the supercapacitor. When discharging back to 0 V, the adsorbed CO_2 is released. In contrast to previous work[13–16], here we employed YP50-F activated carbon, demonstrating that electrochemical CO_2 adsorption by supercapacitors is not limited to the previously studied BPL activated carbon.

Based on the measured pressure changes and the calibrated gas reservoir volume (see Supplementary Information), for negative charging we obtain a CO_2 adsorption capacity of 50 ± 1 mmol kg^{-1} (calculated per kg of carbon in the gas exposed electrode, error bars represent cycle to cycle variation on a single cell). This value is comparable to the 62 ± 3 mmol kg^{-1} reported for a similar SSA system by Zhu et al.[16] We obtained an energy consumption of 628 ± 12 kJ mol^{-1} of adsorbed CO_2, which is larger than the previously reported consumption for SSA (202 ± 14 kJ mol^{-1})[16] or membrane capacitive deionization (27 kJ mol^{-1})[11] systems. The performance is likely hindered by the non-optimized nature of the SSA system in this study, and its relatively high resistance (the equivalent series resistance of this cell was 939 ± 8 Ω).

When then charging the same cell positively (Figure 2b), the adsorption capacity increases significantly to 75 ± 1 mmol kg^{-1} and the energy consumption decreases to 356 ± 17 kJ mol^{-1}. When examining the gas adsorption data for insights to this difference (Figure 2a, 2b), variations in the adsorption behavior are obvious. When charging negatively to –1.0 V the cell adsorbs CO_2 (decreasing reservoir pressure, Figure 2a), but when charging positively to +1.0 V the cell desorbs CO_2 (increasing pressure, Figure 2b); the different charging polarities have opposite effects on gas adsorption. An equivalent statement is that decreasing the cell voltage always causes CO_2 adsorption and increasing the voltage always causes desorption, regardless of the absolute voltage. This implies that the limiting voltages can be chosen arbitrarily, rather than one limit always being 0 V. We therefore hypothesized that we could increase the adsorption capacity by combining the positive and negative charging protocols into a "switching" protocol, with –1 and +1 V as voltage limits.

Excitingly, the switching protocol (Figure 2c) gives an even higher adsorption capacity of 112 ± 7 mmol kg^{-1}, which is significantly larger than the capacity observed for the conventional negative charging protocol (50 ± 1 mmol kg^{-1}), as well as our positive charging protocol (75 ± 2 mmol kg^{-1}). One limitation of this new approach, however, is the increased energy consumption (751 ± 31 kJ mol^{-1}). We predict that further optimization of (i) the SSA device (to reduce resistance) and (ii) the charging protocol will lead to significantly lower energy consumption values in the future. Interestingly the shape of the adsorption profile for the switching protocol differs to that of negative and positive charging protocols, suggesting a change in the underlying capture mechanism.

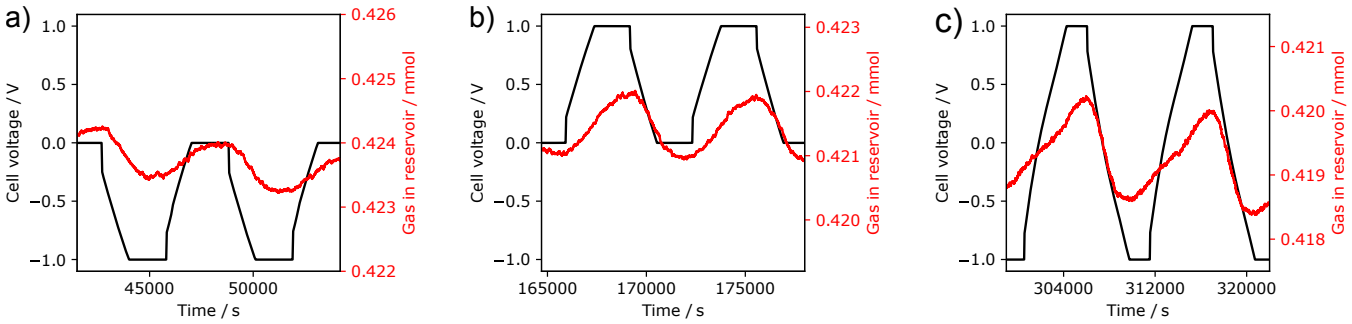

Figure 2. Gas adsorption data from application of a negative (a) or positive (b) voltage between the gas-exposed and counter electrodes, as well as from changing the applied voltage between positive and negative (c). Conducted with 1 M NaCl (aq) electrolyte, 15 mg electrodes, and 30 mA g^{-1} current density.

The relative performances of these different charging protocols are consistent between independent electrochemical cells, though we observe some variation in the magnitudes of the adsorption capacities from cell to cell. The above results are from a cell that was first charged negatively, then charged positively, and finally charged with the switching protocol (Figure S1). When instead applying a positive, then negative, then switching voltage, to an independent cell (Figure S2), we obtain adsorption capacities of 66 ± 4, 38 ± 4, and 97 ± 2, respectively. Very similar results were obtained when the experiments were repeated on two further cells by another researcher (Figures S3 and S4, tables S1 and S2). Finally, we observed some irreversible pressure decreases over the course of our experiments (Figures S1-S4). This may be due to irreversible electrochemical processes such as corrosion, and suggests that further device and material optimization are needed for practical applications.

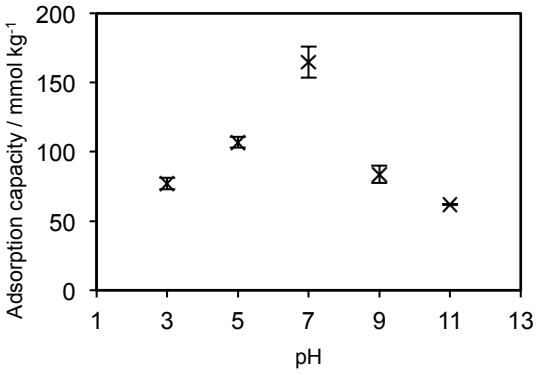

Figure 3. Effects of electrolyte pH on CO_2 adsorption capacity when applying a positive cell voltage. Electrolytes contained NaCl, HCl, NaOH to achieve $[Cl^-]$ = 1 M and the desired pH. Error bars represent cycle-to-cycle variation for a single cell.

The above results highlight an asymmetry in behavior depending on whether the positive or negative electrode is exposed to the gas. Obvious candidates for the ions involved in the electrochemical capture process are HCO_3^-, H^+, and to a lesser extent CO_3^{2-} ions formed from dissolution of CO_2 in water. In addition to their different masses and radii (which affect diffusivity), the different charges on these ions result in varying behavior at the two electrodes.

To examine the role of these ions, we explored the effect of varying electrolyte pH on adsorption capacity. Aqueous electrolytes were made with pHs of 3, 5, 7, 9, and 11, by combining NaCl with HCl or NaOH to achieve both the desired pH and a constant Cl^- concentration of 1 M. The Cl^- concentration was held constant because anions have been reported to be more important than cations for SSA.[15] The greatest adsorption capacity was obtained at pH 7, dropping off with both high and low pHs. This effect was observed both for negative (Figure 3) and positive (Figure S5) charging.

These results imply that HCO_3^- ions are particularly important to the SSA mechanism, since pH 7 gives the highest HCO_3^- concentration: at low pHs, most dissolved carbon dioxide remains as CO_2 or H_2CO_3, and at higher pHs most carbon is present as CO_3^{2-}.[18] It is only in the intermediate regime, where HCO_3^- ions predominate, that maximal adsorption capacity is achieved.

A limitation of this experiment is the lack of measurement of the actual pH during cell operation. The listed values were accurate when the solution was first made, but as electrochemical experiments progress this will change due to (i) CO_2 dissolution which causes pH decreases,[20,21] and (ii) any selective H^+ adsorption by the carbon surface which may increase the pH. The pH in electrode micropores may also vary significantly from the bulk solution, and even between different pores.[18] Further study is therefore important before making firm conclusions regarding pH effects.

The previously proposed mechanisms[14,16] for SSA struggle to account for our new observations, and we therefore outline a new mechanism to rationalize the results. The mechanism must account for the key findings that CO_2 adsorption is observed for negative charging (Figure 2a) and CO_2 desorption is observed

for positive charging (Figure 2b), and that bicarbonate is a key CO_2-derived species. Given that a supercapacitor is a symmetric electrochemical cell, one would initially anticipate identical CO_2 adsorption whether charging positively or negatively. However, our cell design (Figure 1) breaks the cell symmetry, placing one electrode in closer contact with the CO_2 gas reservoir. In our hypothesized mechanism, we therefore focus on the gas-exposed electrode (Figure 4), and the movement of CO_2 derived species into and out of this electrode when charging.

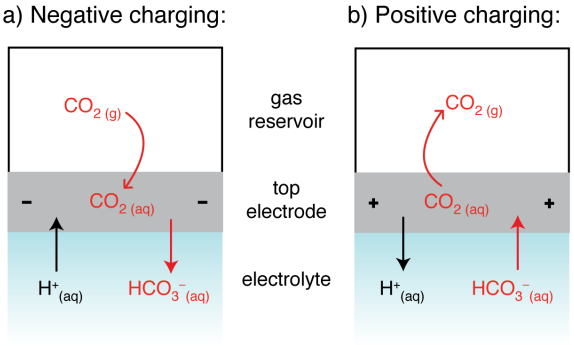

Figure 4. Schematic showing the proposed mechanism for the movement of CO_2 and ions with charging. Other cations (e.g. Na^+) will behave analogously to H^+, and anions (e.g. CO_3^{2-} and Cl^-) to HCO_3^+).

The direction of movement of CO_2 gas observed experimentally is depicted in Figure 4 (by curved red arrows), along with the expected movement of CO_2-derived ions based on charge balancing arguments (straight arrows). For negative charging, we observe that CO_2 adsorbs into the cell during charging. Under these conditions, we anticipate HCO_3^- desorption from the negative electrode.[22] This desorption should reduce the concentration of CO_2 in the negative electrode (since CO_2 and HCO_3^- are in equilibrium), thereby providing a driving force for CO_2 adsorption into the negative electrode. Conversely, for positive charging, the electrosorption of bicarbonate into the positive electrode provides a driving force for CO_2 release. We note electrosorption of H^+ may also impact CO_2 capture,[7,10] though the concentration of these species is expected to be very low at pH 7.

Finally, the electrolyte ions (Na^+ and Cl^-) must also play a significant role in electrochemical CO_2 adsorption. When deionized water is used as an electrolyte in the literature, excluding any supporting electrolyte ions, a somewhat lower adsorption capacity is obtained.[14] We hypothesize that there is either cooperativity or competition between the electrosorption of these ions and the CO_2-derived ions. The electrolyte ions may promote CO_2 adsorption (e.g. via Lewis acid-base interactions) or desorption (perhaps through competition for adsorption sites). The differences in diffusivities between Na^+, Cl^-, H^+, and HCO_3^- further complicates this issue. Ultimately, more experimental and theoretical work must be done to fully unravel the mechanisms of electrochemical CO_2 capture by supercapacitors.

Overall, this study has shown that simple changes to charging protocols can significantly increase the adsorption capacities of supercapacitive swing adsorption. Charging with the positive electrode exposed to gas increases adsorption capacity and decreases energy consumption, and a "switching" protocol further increases capacity. This moves SSA further towards the performance required for commercial viability. It also brings new insights into the mechanism of CO_2 capture, and we propose a new model to account for supercapacitive swing adsorption.

Supplementary Information

Supplementary Information is available with experimental methods, and additional electrochemical gas adsorption data (PDF).

Author Contributions

Conceptualization: A.C.F., T.B.B.
Methodology: T.B.B., G.M., I.T., A.C.F.
Investigation: T.B.B., G.M.
Analysis: T.B.B., G.M., I.T., A.C.F.
Writing – original draft: T.B.B.
Writing – review and editing: T.B.B., G.M., I.T., A.C.F.
Funding acquisition: A.C.F.

Conflicts of Interest

There are no conflicts to declare.

ACKNOWLEDGMENT

This project was supported by a UKRI Future Leaders Fellowship to A.C.F. (MR/T043024/1), and the Yusuf Hamied Department of Chemistry at Cambridge for the award of a BP Next Generation Fellowship to A.C.F. This work was further supported by the NanoDTC Cambridge EP/S022953/1. We thank Prof. Michael De Volder and Dr Céline Merlet for helpful discussions, and Prof. Clare Grey for support to I. T. We also thank the mechanical workshop in the Dept. of Chemistry for preparation of gas cells. A.C.F. thanks Dr Kristian Knudsen and Prof. Bryan McCloskey for helpful discussions and help with feasibility tests at U. C. Berkeley.

REFERENCES

(1) Global Warming of 1.5 C. An IPCC Special Report on the Impacts of Global Warming of 1.5 C above Pre-Industrial Levels and Related Global Greenhouse Gas Emission Pathways, in the Context of Strengthening the Global Response to the Threat of Climate Change, Sustainable Development, and Efforts to Eradicate Poverty; Masson-Delmotte, V., Zhai, P., Portner, H.-O., Roberts, D., Skea, J., Shukla, P. R., Pirani, A., Moufouma-Okia, W., Pean, C., Pidcock, R., Connors, S., Matthews, J. B. R., Chen, Y., Zhou, X., Gomis, M. I., Lonnoy, E., Maycock, T., Tignor, M., Waterfield, T., Series Eds.; IPCC, 2018.

(2) Gielen, D.; Boshell, F.; Saygin, D.; Bazilian, M. D.; Wagner, N.; Gorini, R. The Role of Renewable Energy in the Global Energy Transformation. Energy Strategy Rev. **2019**, 24, 38–50. https://doi.org/10.1016/j.esr.2019.01.006.

(3) Bataille, C. G. F. Physical and Policy Pathways to Net-Zero Emissions Industry. WIREs Clim. Change **2020**, 11 (2), e633. https://doi.org/10.1002/wcc.633.

(4) Committee on Climate Change. Net Zero: The UK's Contribution to Stopping Global Warming; Technical report; Committee on Climate Change, 2019.

(5) Rochelle, G. T. Amine Scrubbing for CO2 Capture. Science **2009**, 325 (5948), 1652–1654. https://doi.org/10.1126/science.1176731.

(6) Al-Mamoori, A.; Krishnamurthy, A.; Rownaghi, A. A.; Rezaei, F. Carbon Capture and Utilization Update. Energy Technol. **2017**, 5 (6), 834–849. https://doi.org/10.1002/ente.201600747.

(7) Rahimi, M.; Catalini, G.; Puccini, M.; Alan Hatton, T. Bench-Scale Demonstration of CO 2 Capture with an Electrochemically Driven Proton Concentration Process. RSC Adv. **2020**, 10 (29), 16832–16843. https://doi.org/10.1039/D0RA02450C.

(8) Renfrew, S. E.; Starr, D. E.; Strasser, P. Electrochemical Approaches toward CO2 Capture and Concentration. ACS Catal. **2020**, 10 (21), 13058–13074. https://doi.org/10.1021/acscatal.0c03639.

(9) Kang, J. S.; Kim, S.; Hatton, T. A. Redox-Responsive Sorbents and Mediators for Electrochemically Based CO2 Capture. Curr. Opin. Green Sustain. Chem. **2021**, 31, 100504. https://doi.org/10.1016/j.cogsc.2021.100504.

(10) Jin, S.; Wu, M.; Gordon, R. G.; Aziz, M. J.; Kwabi, D. G. PH Swing Cycle for CO2 Capture Electrochemically Driven through Proton-Coupled Electron Transfer. Energy Environ. Sci. **2020**, 13 (10), 3706–3722. https://doi.org/10.1039/D0EE01834A.

(11) Legrand, L.; Schaetzle, O.; de Kler, R. C. F.; Hamelers, H. V. M. Solvent-Free CO2 Capture Using Membrane Capacitive Deionization. Environ. Sci. Technol. **2018**, 52 (16), 9478–9485. https://doi.org/10.1021/acs.est.8b00980.

(12) Voskian, S.; Hatton, T. A. Faradaic Electro-Swing Reactive Adsorption for CO2 Capture. Energy Environ. Sci. **2019**, 12 (12), 3530–3547. https://doi.org/10.1039/C9EE02412C.

(13) Kokoszka, B.; Jarrah, N. K.; Liu, C.; Moore, D. T.; Landskron, K. Supercapacitive Swing Adsorption of Carbon Dioxide. Angew. Chem. Int. Ed. **2014**, 53 (14), 3698–3701. https://doi.org/10.1002/anie.201310308.

(14) Zhu, S.; Li, J.; Toth, A.; Landskron, K. Relationships between Electrolyte Concentration and the Supercapacitive Swing Adsorption of CO2. ACS Appl Mater Interfaces **2019**, 7.

(15) Zhu, S.; Li, J.; Toth, A.; Landskron, K. Relationships between the Elemental Composition of Electrolytes and the Supercapacitive Swing Adsorption of CO_2. ACS Appl. Energy Mater. **2019**, 2 (10), 7449–7456. https://doi.org/10.1021/acsaem.9b01435.

(16) Zhu, S.; Ma, K.; Landskron, K. Relationships between the Charge–Discharge Methods and the Performance of a Supercapacitive Swing Adsorption Module for CO2 Separation. J. Phys. Chem. C **2018**, 122 (32), 18476–18483. https://doi.org/10.1021/acs.jpcc.8b03968.

(17) E. Boot-Handford, M.; C. Abanades, J.; J. Anthony, E.; J. Blunt, M.; Brandani, S.; Dowell, N. M.; R. Fernández, J.; Ferrari, M.-C.; Gross, R.; P. Hallett, J.; Stuart Haszeldine, R.; Heptonstall, P.; Lyngfelt, A.; Makuch, Z.; Mangano, E.; J. Porter, R. T.; Pourkashanian, M.; T. Rochelle, G.; Shah, N.; G. Yao, J.; S. Fennell, P. Carbon Capture and Storage Update. Energy Environ. Sci. **2014**, 7 (1), 130–189. https://doi.org/10.1039/C3EE42350F.

(18) Legrand, L.; Shu, Q.; Tedesco, M.; Dykstra, J. E.; Hamelers, H. V. M. Role of Ion Exchange Membranes and Capacitive Electrodes in Membrane Capacitive Deionization (MCDI) for CO2 Capture. J. Colloid Interface Sci. **2020**, 564, 478–490. https://doi.org/10.1016/j.jcis.2019.12.039.

(19) Temprano, I.; Liu, T.; Petrucco, E.; Ellison, J. H. J.; Kim, G.; Jónsson, E.; Grey, C. P. Toward Reversible and Moisture-Tolerant Aprotic Lithium-Air Batteries. Joule **2020**, 4 (11), 2501–2520. https://doi.org/10.1016/j.joule.2020.09.021.

(20) McBain, J. W. The Use of Phenolphalein as an Indicator. The Slow Rate of Neutralisation of Carbonic Acid. J. Chem. Soc. Trans. **1912**, 101, 814–820.

(21) Loerting, T.; Bernard, J. Aqueous Carbonic Acid (H2CO3). ChemPhysChem **2010**, 11 (11), 2305–2309. https://doi.org/10.1002/cphc.201000220.

(22) Forse, A. C.; Merlet, C.; Griffin, J. M.; Grey, C. P. New Perspectives on the Charging Mechanisms of Supercapacitors. J. Am. Chem. Soc. **2016**, 138 (18), 5731–5744. https://doi.org/10.1021/jacs.6b02115.

Supplementary Information for:

Enhancing the capacity of supercapacitive swing adsorption CO_2 capture by tuning charging protocols and pH

Trevor B. Binford, Grace Mapstone, Israel Temprano, Alexander C. Forse*

Experimental Methods

Device construction. Electrochemical gas adsorption experiments were carried out with a custom made device (Figure 1). A symmetric supercapacitor with 1 M NaCl (aq.) electrolyte was sandwiched between a bottom current collector and a titanium mesh contacting a top current collector, while the volume above the mesh was filled with pure CO_2 gas (Sigma Aldrich 99.9 atom% ^{12}C). A potentiostat (Biologic, VSP-3e) attached to the two current collectors applied a potential across the electrodes to charge the supercapacitor. By monitoring the gas reservoir with a pressure transducer (Omega, PX309-030A5V), we measured the CO_2 taken up or released by the SSA effect. Titanium was used for the current collectors and mesh to minimize corrosion. Chloride ions are particularly corrosive, so stainless steel is unsuitable for material in contact with the NaCl electrolyte.

Preparation of carbon films. All electrodes were made from activated carbon (YP-50F, Kuraray, which was found to perform favorably compared to activated carbons used in the literature) and polytetrafluoroethylene (PTFE, 60% wt. dispersion in water, Aldrich) mixed in a ratio of 95:5 by weight. The PTFE serves as a binder to hold together the electrode and make it more malleable for rolling out into a film. First, activated carbon was dispersed in several mL of ethanol in an ultrasonic bath, then mixed with the PTFE dispersion on a watch-glass. The mixture was continually stirred with a spatula to ensure through mixing. As the ethanol evaporated, drying portions of the mixture were gathered into a single mass, until enough ethanol evaporated that the collected carbon and PTFE had a dough-like consistency. After kneading and adding additional ethanol as necessary to achieve the desired consistency, the carbon was transferred to a glass sheet and rolled to a uniform thickness with a steel rolling pin. The material was then transferred with a razor blade to aluminum foil, which was folded into a wallet and placed into a vacuum oven overnight at 80-100 °C to remove residual ethanol/water.

After drying, circular electrodes were cut from the carbon film using a steel punch (0.5 inch diameter). Each electrode was cut to achieve a mass within 10% of 15 mg, and trimmed down if necessary (e.g. due to uneven film thickness). The mass of each electrode was recorded three times, with the mass recorded as the mean of the measurements and the error as the deviation from that mean. Filter paper (Whatman 55 mm Cat No. 1001-055) was used for a separator, cut into a circle slightly less than the diameter of the current collector. This minimized chances of a short circuit, such as from a misaligned electrode or bending titanium mesh contacting the opposite current collector.

Before assembly of the device, the electrodes were soaked to ensure good wetting and infiltration of the electrolyte into the activated carbon micropores. Either both electrodes (cells A1 and A2) or only the bottom electrode (cells B1 and B2, as well as the cells used in the pH variation experiment in Figures 3 and S5) were soaked for 2 hours. In the case of the cells with only one soaked electrode, the soaked electrode was used in the bottom, non-gas exposed, side. For cells B1 and B2 the separator was soaked alongside the bottom electrode. For cells A1, A2 and the cells for the pH study (Figures 3 and S5), the separator was only briefly soaked in electrolyte (for a few seconds) before assembly. Qualitatively similar results were obtained with both symmetric and asymmetric soaking (see figures and tables below).

Electrochemical gas adsorption experiments. The device was charged with a protocol adapted from Zhu et al.[1] A constant current (30 mA / g of the gas-exposed electrode) was applied until a target cell potential between the electrodes was reached. This potential was then held for 30 minutes (to give more time to equilibrate), then a 30 mA/g constant current applied to return the system to the initial potential, and a final 30 minute potential holding step. This procedure was repeated for the desired number of cycles.

For each charge/discharge cycle, the amount of CO_2 adsorbed was calculated by taking the difference between the peaks and troughs of the amount of gas in the reservoir. This was calculated from the pressure transducer data (smoothed over a window of 100 seconds) using

the ideal gas equation $pV = nRT$. The volume of the reservoir was calculated during the process of dosing CO_2 into the cell, based on pressure measurements of the added gas (using Boyle's Law $P_1V_1 = P_2V_2$). The cell was kept in a 30 ºC incubator to control the temperature, though the initial temperature increase when first putting into the incubator is associated with the initial rise in the calculated amount of gas in the cell. To account for any linear changes in pressure over time each peak value was compared to the mean of the two adjacent troughs. The amount of gas adsorbed in one cycle was then normalized by the mass of carbon in the gas-exposed electrode to give the adsorption capacity in mmol/kg. The overall adsorption capacity was taken as the mean of adsorption capacities for each cycle, and the error calculated using a 95% confidence interval with the Student's t-test.

Although the calculated metrics were generally consistent from one cycle to the next (within ~10%), there were occasional outlier cycles. These are evident in the gas in reservoir vs time plots as deviations from a smooth, roughly sinusoidal curve. Such outliers are attributed to rapid changes in temperature (due to other activities in the lab) or intermittent leaks in the cell (caused by poor seals, perhaps from corrosion by electrolyte interaction with the metal of the cell). Any results from these cycles were excluded from the analysis above to calculate the reported data.

Supplementary Figures

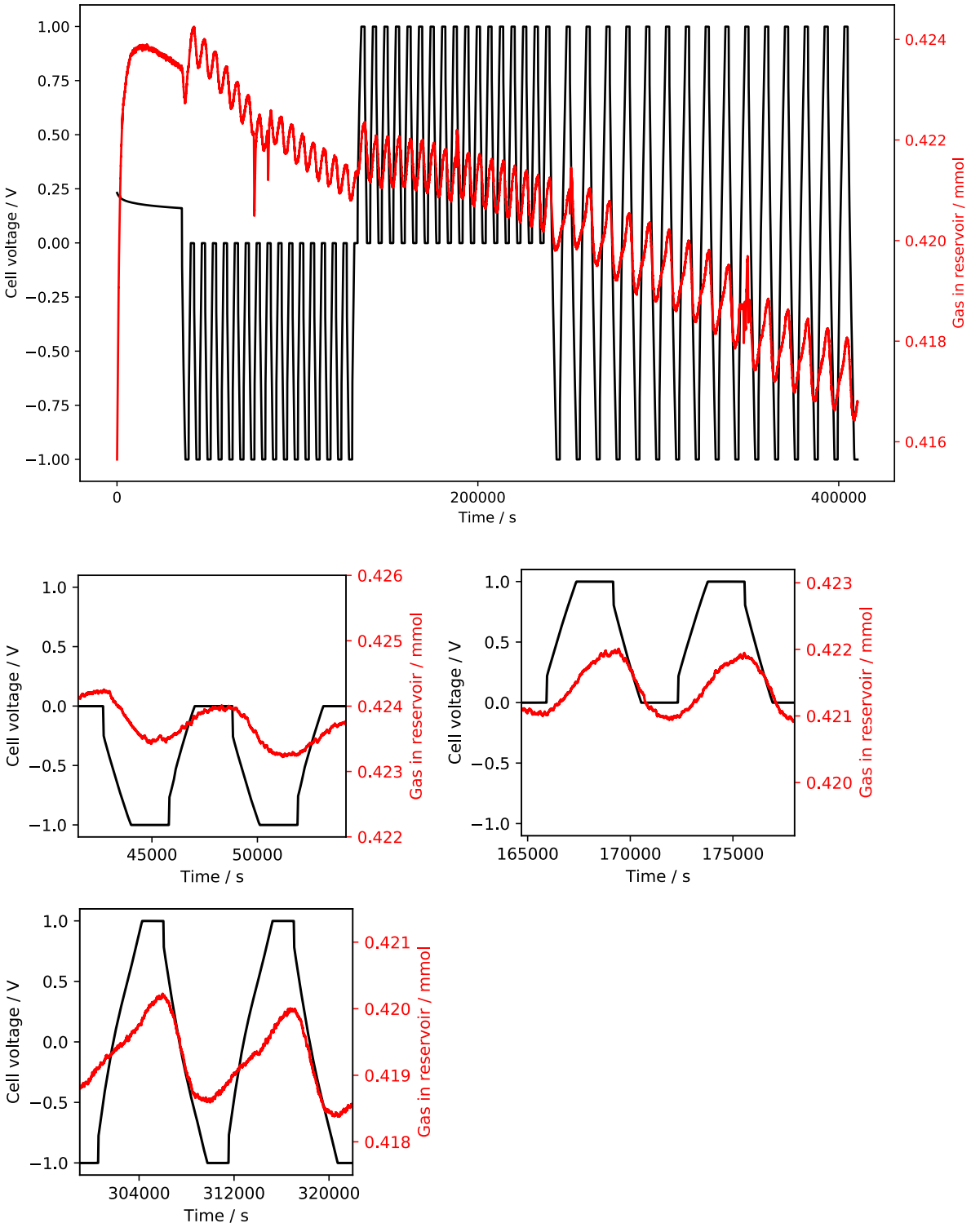

Figure S1. Overall experiment and representative cycles from positive, negative, and switching cycling protocols on cell A1 (same as in main body of this paper). Conducted with 1 M NaCl (aq) electrolyte, 15 mg electrodes, and 30 mA g^{-1} current density. Anomalous peaks presumed to be from short-term temperature changes. In additional to the reversible adsorption, gradual irreversible pressure reductions are observed throughout the experiment, which may arise due to irreversible electrochemical processes such as corrosion.

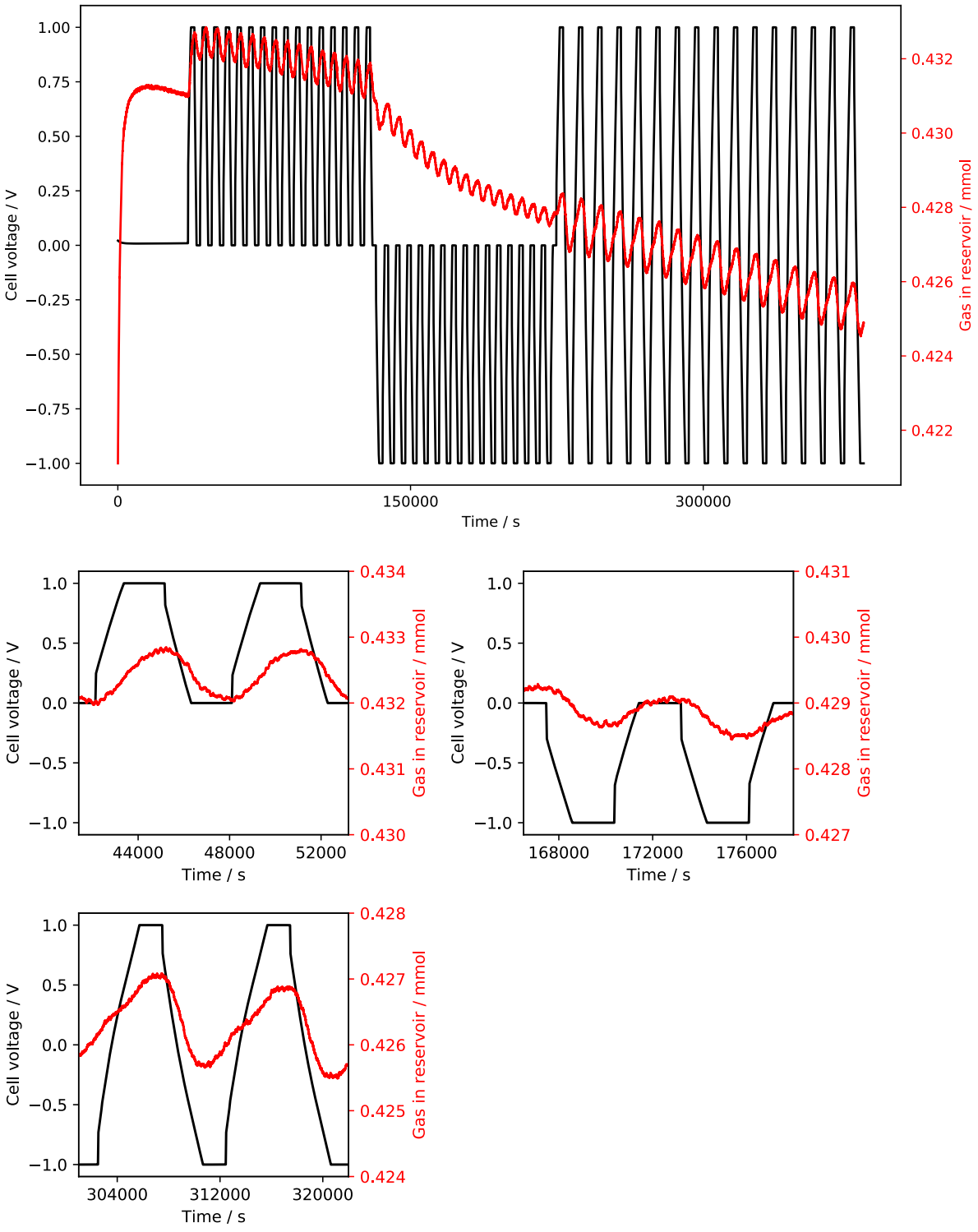

Figure S2. Overall experiment and representative cycles from negative, positive, and switching cycling protocols on cell A2. Conducted with 1 M NaCl (aq) electrolyte, 15 mg electrodes, and 30 mA g^{-1} current density. Anomalous peaks presumed to be from short-term temperature changes.

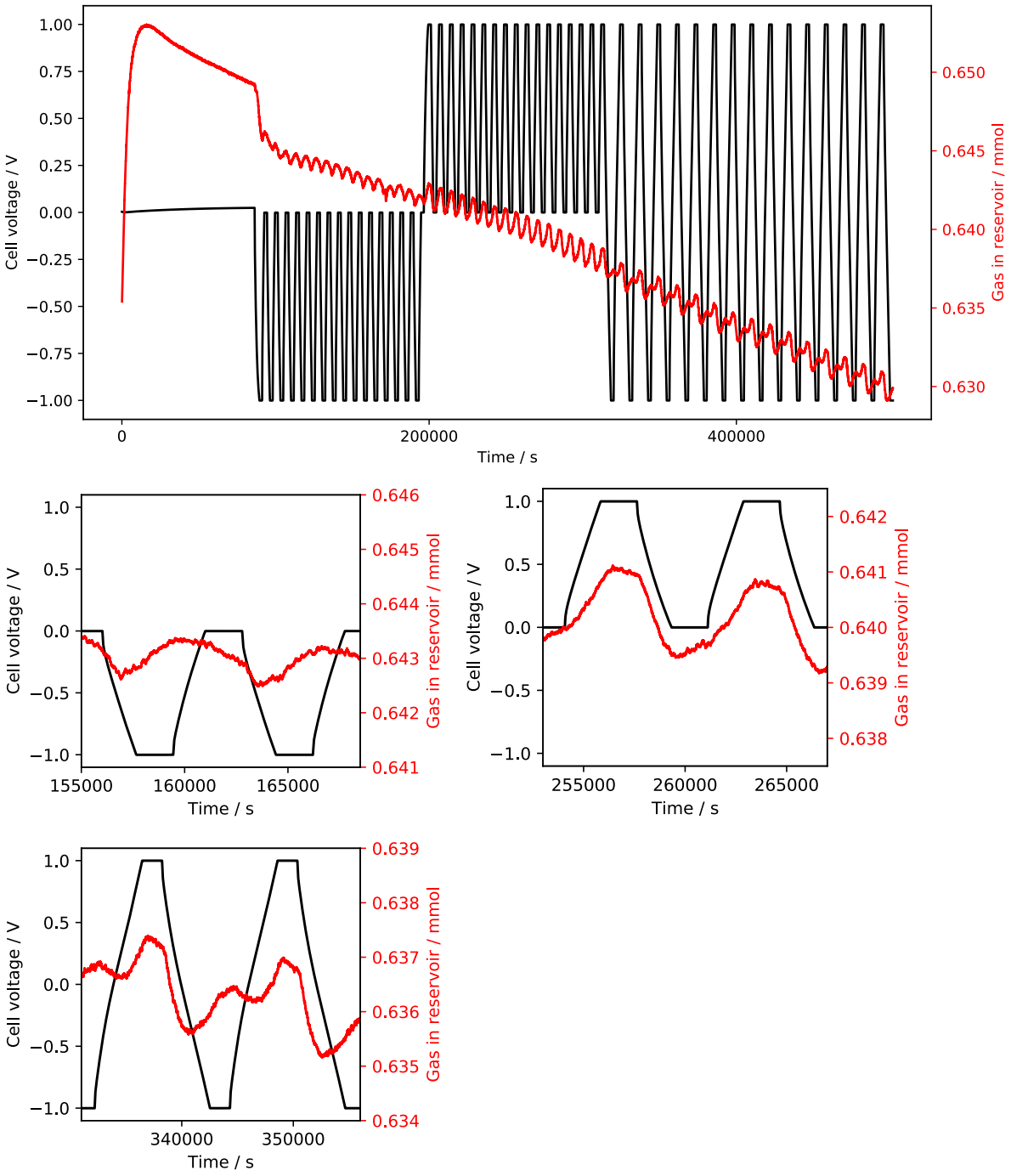

Figure S3. Overall experiment and representative cycles from negative, positive, and switching cycling protocols on cell B1. Conducted with 1 M NaCl (aq) electrolyte, 15 mg electrodes, and 30 mA g^{-1} current density. Anomalous peaks presumed to be from short-term temperature changes. As opposed to cells A1 and A2, only the electrode not directly exposed to the gas was soaked with electrolyte (the gas-exposed electrode was wetted with a few drops of electrolyte).

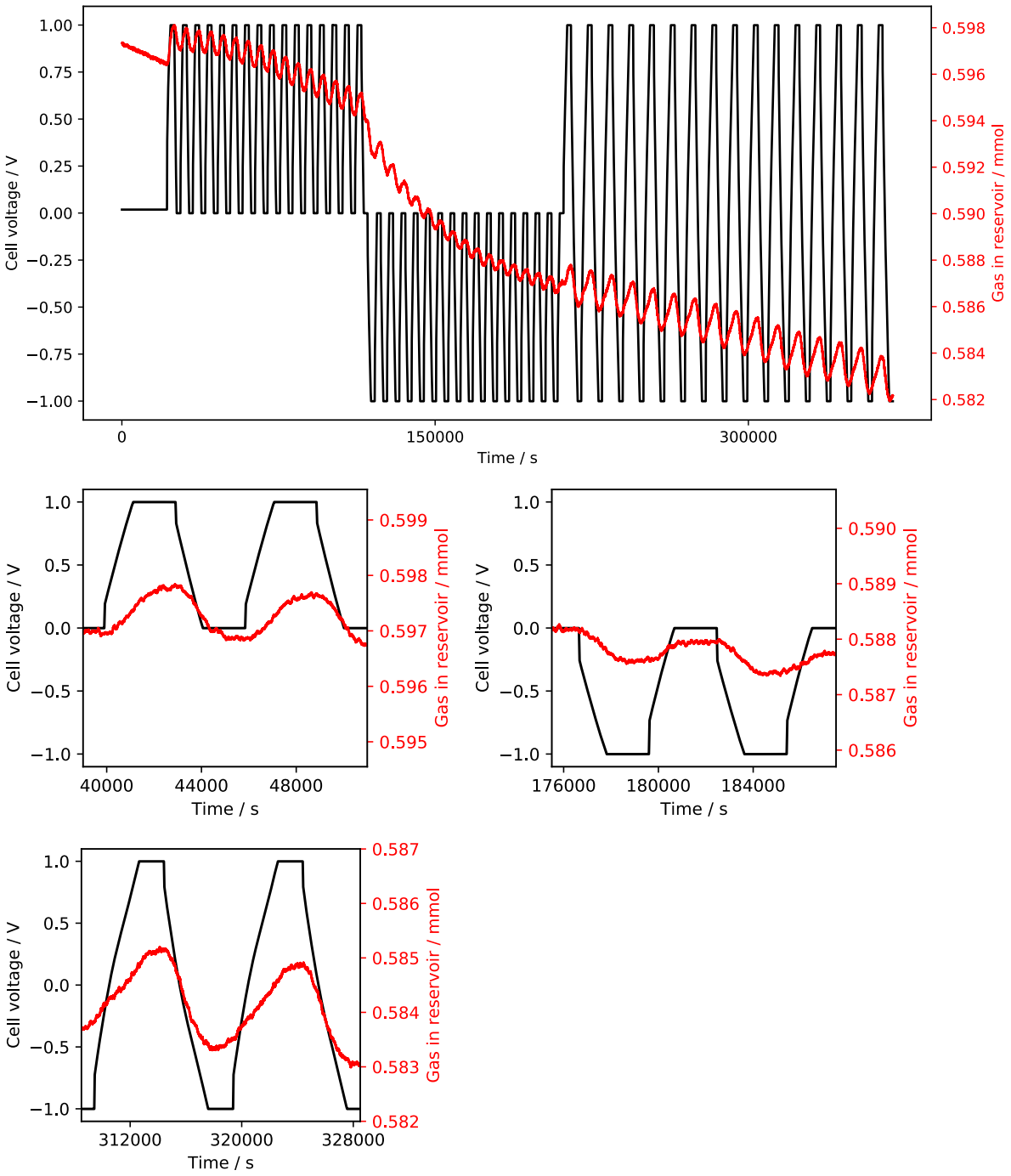

Figure S4. Overall experiment and representative cycles from positive, negative, and switching cycling protocols on cell B2. Conducted with 1 M NaCl (aq) electrolyte, 15 mg electrodes, and 30 mA g^{-1} current density. Anomalous peaks presumed to be from short-term temperature changes. As opposed to cells A1 and A2, only the electrode not directly exposed to the gas was soaked with electrolyte (the gas-exposed electrode was wetted with a few drops of electrolyte).

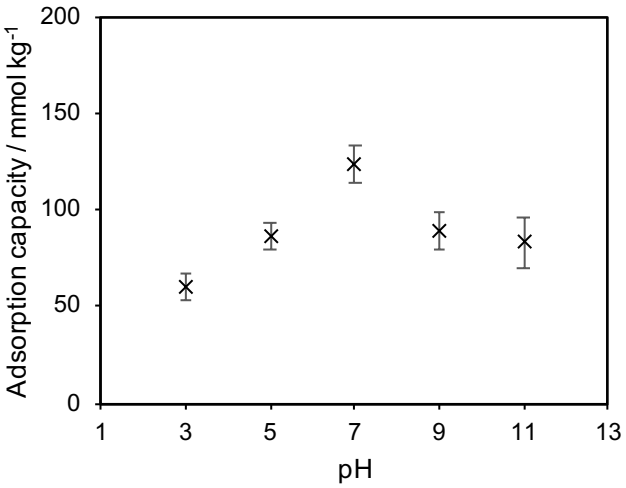

Figure S5. Effects of electrolyte pH on CO_2 adsorption capacity when applying a negative cell voltage. Electrolytes contained NaCl, HCl, NaOH to achieve [Cl^-] = 1 M and the desired pH.

Table S1. Adsorption capacities (in mmol kg^{-1}) and energy consumption (in kJ mol^{-1}) for two cells that were cycled with first a negative charging protocol, then positive, then switching. Each cell was assembled and run by a different researcher to minimize biases. Cell A1 had both electrodes soaked; cell B1 had only electrode not exposed to gas soaked.

Cell	A1		B1	
	Adsorption capacity / mmol kg^{-1}	Energy consumption / kJ mol^{-1}	Adsorption capacity / mmol kg^{-1}	Energy consumption / kJ mol^{-1}
Negative	50 ± 1	628 ± 12	55 ± 5	445 ± 85
Positive	75 ± 1	356 ± 17	108 ± 2	217 ± 22
Switching	112 ± 7	751 ± 39	111 ± 3	596 ± 48

Table S2. Adsorption capacities (in mmol kg^{-1}) and energy consumption (in kJ mol^{-1}) for two cells that were cycled with first a positive charging protocol, then negative, then switching. Each cell was assembled and run by a different researcher to minimize biases. Cell A2 had both electrodes soaked; cell B2 had only electrode not exposed to gas soaked.

Cell	A2		B2	
	Adsorption capacity / mmol kg^{-1}	Energy consumption / kJ mol^{-1}	Adsorption capacity / mmol kg^{-1}	Energy consumption / kJ mol^{-1}
Positive	66 ± 4	348 ± 27	75 ± 2	252 ± 14
Negative	38 ± 4	819 ± 47	48 ± 6	588 ± 43
Switching	97 ± 2	803 ± 20	123 ± 2	621 ± 12

References:

(1) Zhu, S.; Ma, K.; Landskron, K. *J. Phys. Chem. C* **2018**, *122*, 18476–18483.